Failure Mechanism and Seismic Capacity of RC Frames with URM Wall considering Its Diagonal Strut

KW. Jin
The University of Tokyo, Japan

H. Choi, N. Takahashi & Y. Nakano
Institute of Industrial Science, The University of Tokyo, Japan

15 WCEE
LISBOA 2012

SUMMARY
In this study, RC frames with unreinforced concrete block (CB) wall for typical school buildings in Korea are experimentally investigated to evaluate their seismic capacity. For this purpose, one-fourth scale, one-bay specimens with/without CB wall are designed, and in-plane loading tests are carried out. In this paper, the diagonal strut mechanism of CB wall including its main angle, average compressive strain, central axis, and equivalent width is discussed using principal compressive strains on CB wall. The lateral strength carried by CB wall and RC frame is also explained based on the compressive stress acting on CB wall and the curvature distribution along both columns during the test.

Key Words: URM wall, RC building, Principal strain, Diagonal strut, Shear strength

1. INTRODUCTION

In some regions of Asia, Europe, and Latin America where earthquakes frequently occur, serious earthquake damage is commonly found resulting in catastrophic building collapse. Such damaged buildings often have unreinforced masonry (URM) walls, which are considered non-structural elements in the structural design stage, and building engineers have paid less attention to their effects on structural performance although URM walls may interact with boundary frames. The evaluation of seismic capacity of URM walls built in boundary frames is therefore urgently necessary to mitigate earthquake damage for those buildings.

For this purpose, RC frames with unreinforced concrete block (CB) wall for typical school buildings in Korea are experimentally investigated to evaluate their seismic capacity including failure mechanism and load bearing capacity. One-fourth scale, one-bay specimens, which are bare frame specimen and infilled frame specimen, are designed, and their in-plane loading tests are carried out. In this paper, the diagonal strut mechanism of CB wall including its main angle, average compressive strain, central axis, and equivalent width is discussed using the principal compressive strains on CB wall. The shear strength carried by CB wall and RC frame is also explained based on the test results.

2. OUTLINE OF EXPERIMENT

2.1. Prototype Building and Experiment Parameters

The test specimens are designed according to the standard design of Korean 4 story school buildings (referred to as "prototype building" shown in Fig. 1) in the 1980's (The Ministry of Construction and Transportation, 2002). In this study, two specimens which are bare frame (BF) and CB wall infilled frame (IF) having an axial load level of their first story are tested under in-plain loadings. Cyclic loads are employed in BF specimen, while pushover loads are applied in IF specimen to carefully evaluate diagonal strut mechanism from strain gauges attached on CB wall as will be described later.
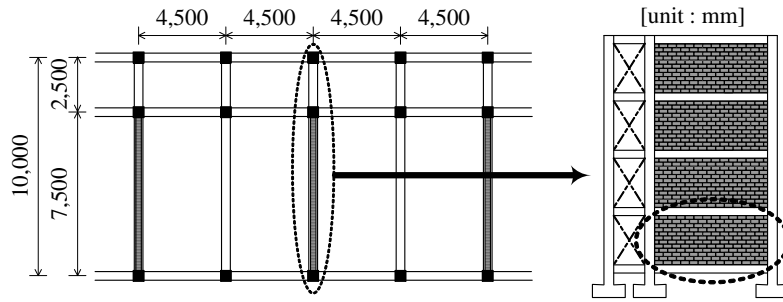
Figure 1. Standard design of Korean 4 story school buildings in the 1980's

2.2. Design of Small-Scale Specimen

Figure 2 shows the BF specimen and the IF specimen. The design detail for each member is briefly described as follows.

2.2.1. Column and beam

The size of column section is 1/4 of that of prototype building. The axial stress in columns, the ratio of longitudinal reinforcement, and that of shear reinforcement are almost the same as the prototype building. As shown in Fig. 2, the upper beam of the specimen is designed rigid enough to remain elastic even after the columns and CB wall fail.

2.2.2. Concrete block units

The concrete block unit is 1/4 of that of the full-scale unit. It has three hollows inside and a half-sized hollow on each end as shown in Fig. 3 and Photo 1. The cement-to-sand ratio is adjusted so that the strength and stiffness of three layered CB prism specimens should be close to those of the full-scale.
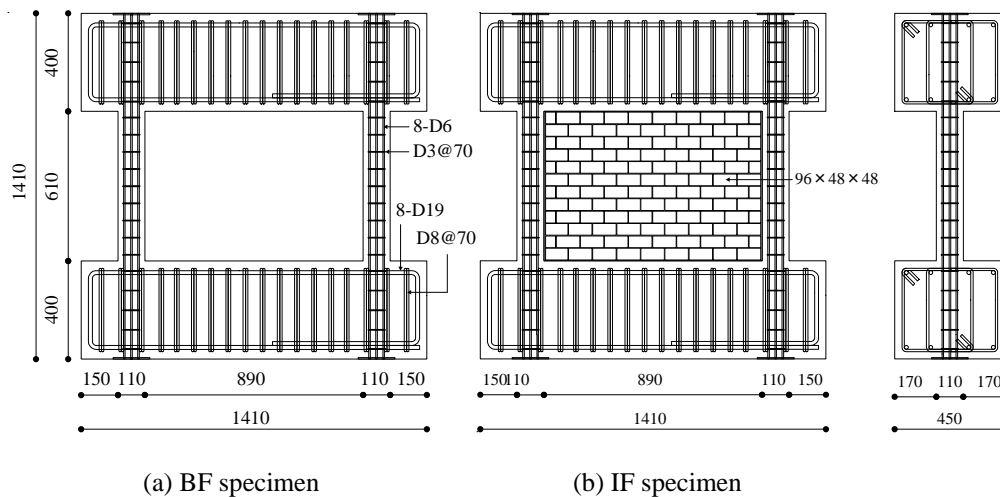

(a) BF specimen   (b) IF specimen
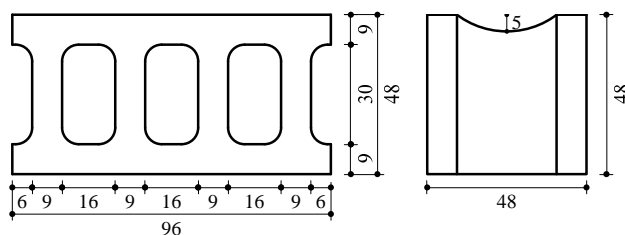**Figure 2.** Details of specimens (unit:mm)

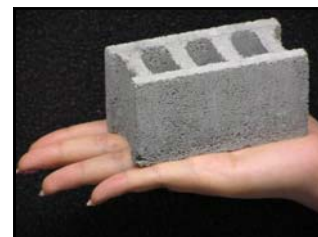**Figure 3.** Details of small scale CB unit (unit : mm)   **Photo 1:** Small scale CB unit

Table 1. Mechanical properties of concrete (Mean value of 3 samples)

Compressive strength	Elastic modulus	Split tensile strength
29MPa	2.1×10^4MPa	2.4MPa

Table 2. Mechanical properties of reinforcement (Mean value of 3 samples)

Bar	Use / Member	Yield strength	Tensile strength	Young's modulus
D3 (SD390)	Hoop / Column	425MPa	495MPa	1.9×10^5MPa
D6 (SD345)	Main bar / Column	371MPa	525MPa	2.1×10^5MPa

Table 3. Mechanical properties of concrete block (Mean value of 3 samples)

| Concrete Block Prism*	
Compressive strength	Young's modulus
6.5 (7.3)MPa	$1.1 (2.0) \times 10^4$MPa

* 3 layered specimen, (   ) : Material test results of full-scale CB unit

2.3. Material Characteristic

Tables 1 through 3 show the material test results, where the values represent the mean value of 3 samples in each test. Although the design strength of concrete specified in the standard design of Korean school buildings in the 1980's is 21 MPa, the compressive strength of test pieces exceeds it as shown in Table 1. The yield strength of reinforcement shows higher values by 5 to 20% than the nominal strength. The compressive strength and Young's modulus from the 3 layered CB prism tests are around 90% and 60% of the full-scale CB prism, respectively. Although the Young's modulus of CB prism is not reproduced, it is found through previous investigations (FEMA 306, 1998) that the reduction of Young's modulus does not have much effect on the shear strength Vc of CB wall, and those 1/4-scale CB units are therefore applied to the test specimen.

2.4. Loading Program

The loading system of IF specimen is shown in Fig. 4. Pushover lateral loads are employed in IF specimen, while cyclic lateral loads are applied to BF specimen through the loading beam tightly fastened to the specimen. Peak drift angles of 0.1, 0.2, 0.4, 0.67, 1.0, 1.5, 2.0, and 3.0% are planned, and 2.5 cycles for each peak drift are imposed to BF specimen to be consistent with the loading plan of other IF specimens to be tested in the near future, where the 2.5 cycle loadings will be applied to eliminate one-sided progressive failure (unsymmetric failure pattern in positive and negative loadings). Herein, a peak drift angle (R) is defined as "lateral deformation (δ) / column height (h_0=610mm)". It should also be noted that 0.4% loading is imposed after 1.0% to investigate the effect of small amplitude loading (i.e., aftershocks) after large deformation for BF specimen. A constant axial load of 96kN (4.0MPa) is applied to each specimen.
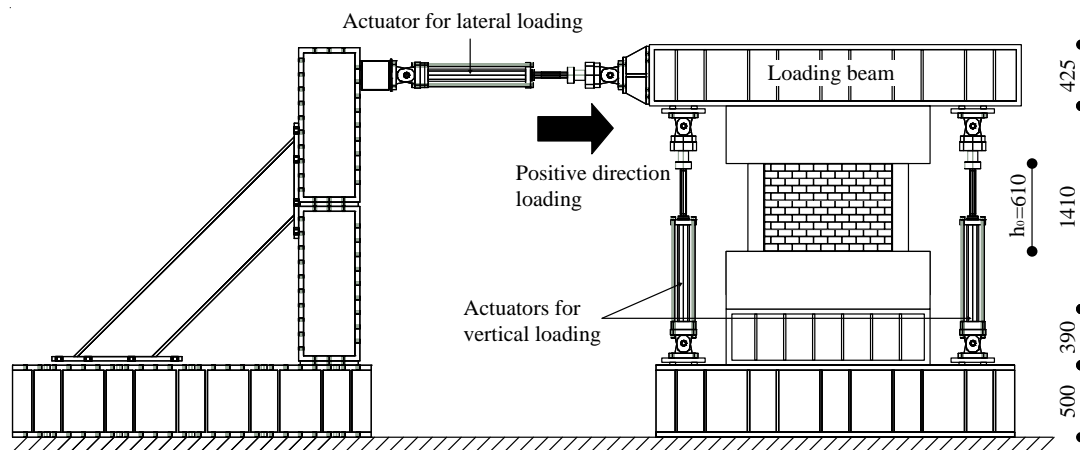
Figure 4. Test setup of IF specimen (Unit:mm)

2.5. Instrumentation

The measurement system of IF specimen is shown in Fig. 5. The relative lateral displacement between upper and lower beams, the vertical displacement of each column, and the diagonal deformation of frame are measured. To measure the curvature distribution in columns, displacement transducers (LVDTs) are set up on both sides of each column at an interval of 150mm. A three-axis strain gauge, which is attached on each CB unit (114 units) to estimate the equivalent strut width and the shear strength of CB wall, is the key point of this measurement plan. Strains of longitudinal and shear reinforcement in columns are also measured. The measurement of BF specimen is consistent with that of IF specimen except CB wall.
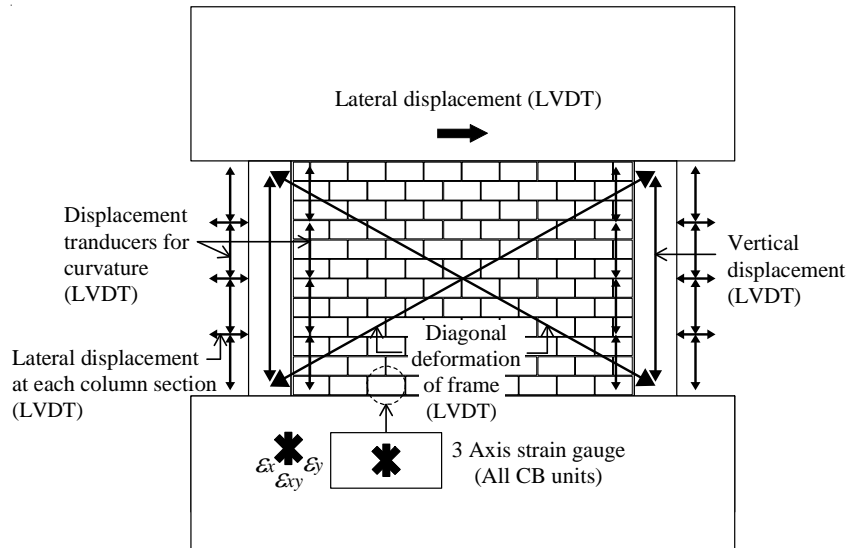

Figure 5. Instrumentation of IF specimen

3. TEST RESULTS

Figure 6 shows the relationship between lateral strength and drift angle. Figure 7 shows the crack patterns in each specimen at the peak drift angle of 2.0% and 1.5%, respectively.

3.1. BF specimen

As shown in Fig. 6(a) and Fig. 7(a), flexural cracks in tensile column and in compression column are observed at the drift angle of 0.065% and 0.2%, respectively. A shear crack in tensile column is observed during 0.4% loading, and the compression column has a shear crack at the drift angle of 0.67%. The longitudinal reinforcement in columns also yields at around this drift angle. The lateral strength gradually increases until 2.0% loading, and the maximum strength of 34.5kN is recorded. Finally, shear cracks at the top of tensile column and the bottom of compression column rapidly open at the drift angle of 3.0%, resulting in sudden deterioration of the lateral load carrying capacity.

In order to calculate the lateral strength of BF specimen, which is shown in Fig. 6(a), the initial stiffness (K_c), secant stiffness ($\alpha_y \cdot K_c$), and cracking moment (M_c) of columns are calculated according to the Eqns. (1) through (3) (AIJ, 2010). The ultimate bending moment M_u of columns is also calculated based on the plane-section assumption setting the ultimate strain ε_{cu} at the compression fiber of concrete equal to 0.003 with an equivalent rectangular stress block coefficient 0.85 (AIJ, 1988). The observed curvature distribution and the assumed moment distribution in both columns are shown in Fig. 8. The overall lateral strength from the calculation result then shows good agreement with the test result as shown in Fig. 6(a).

$$K_c = (h_0^3 / 12EI + \kappa h_0 / GA)^{-1} \tag{1}$$

$$\alpha_y = (0.043 + 1.64np_t + 0.43a/D + 0.33\eta_0) \cdot \left(\frac{d}{D}\right)^2 \tag{2}$$

$$M_c = 0.56\sqrt{\sigma_B} Z_e + ND/6 \tag{3}$$

where, h_0 is the column height, E is the Young's modulus of concrete, I is the moment of inertia of column, κ is the shape factor, G is the shear modulus, A is the column section area, n is the ratio of Young's modulus, p_t is the tension reinforcement ratio, a/D is the shear span ratio, d is the effective column width, D is the column width, σ_B is the concrete strength, Z_e is the section modulus of column, and N is the axial force, respectively.

3.2. IF specimen

As shown in Fig. 6(b) and Fig. 7(b), IF specimen has vertical and horizontal cracks in joint mortar between CB units at the drift angle of 0.05%, and a flexural crack in tensile column occurs at the drift angle of 0.06%. During 0.1% loading, stair-stepped cracks in the CB wall are observed, and the remaining part of CB wall (enclosed by a dashed line in Fig. 7(b)) behaves as a partial height wall restraining the lateral deformation of tensile column, which results in early yielding of longitudinal reinforcement in tensile column (at around the drift angle of 0.27%). Clear shear cracks at the top of tensile column and the bottom of compression column are observed at the peak drift angle of 0.4% and 0.67%, respectively. The maximum strength of 68.5kN is recorded at the drift angle of 0.7% shortly after the longitudinal reinforcement in compression column yields. No remarkable strength deterioration is observed until the drift angle of 1.8%, but a sudden shear failure occurs resulting in rapid opening of shear cracks at the top of tensile column and the bottom of compression column at this drift angle.
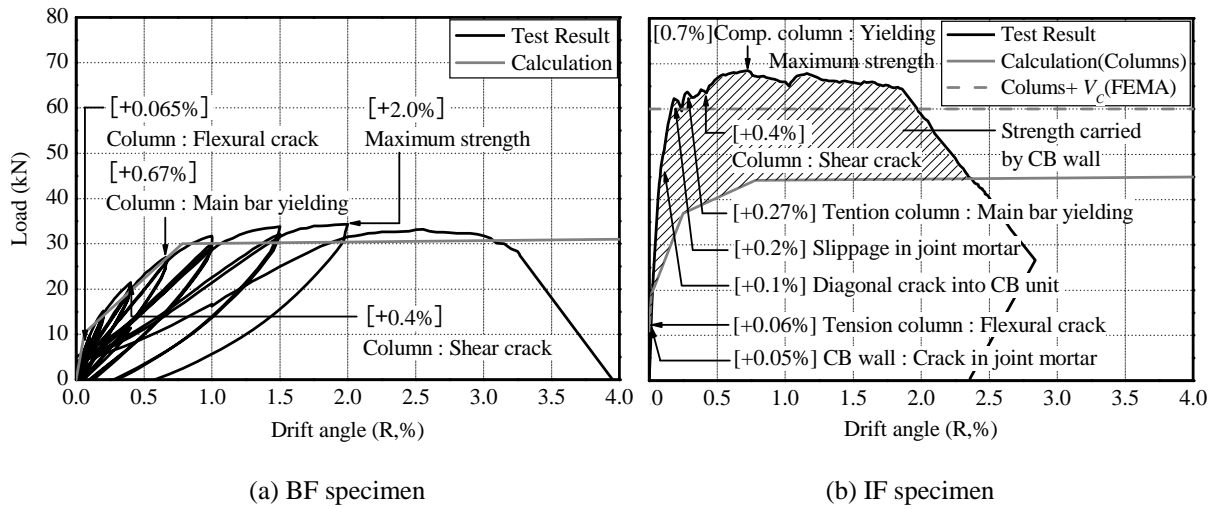

(a) BF specimen   (b) IF specimen

Figure 6. Lateral strength and drift angle relation

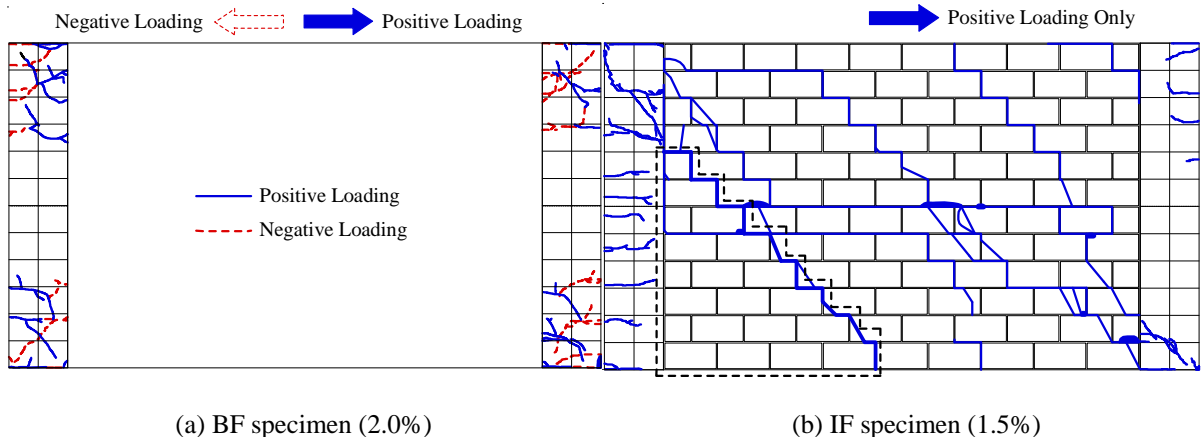(a) BF specimen (2.0%)   (b) IF specimen (1.5%)

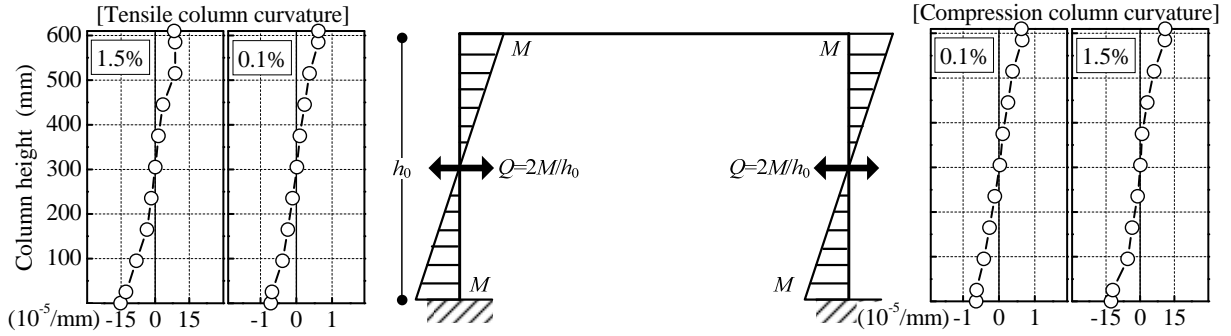**Figure 7.** Crack patterns in both specimen

Figure 8. Curvature and moment distribution of Columns assumed in BF specimen
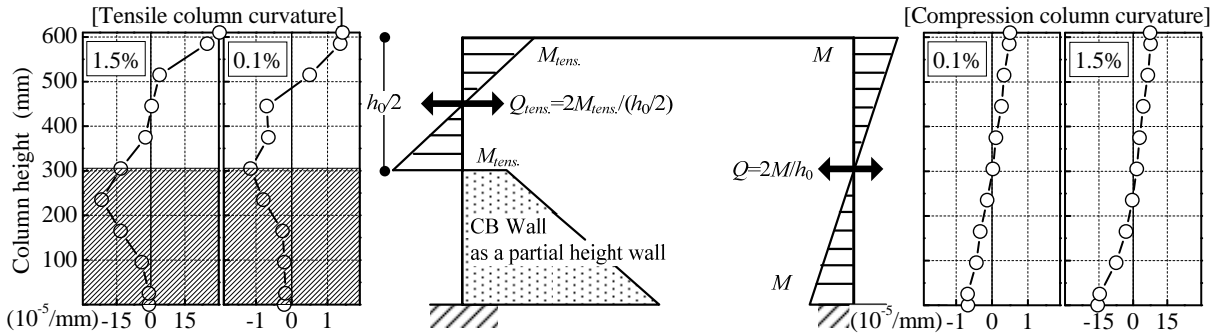

Figure 9. Curvature and moment distribution of Columns assumed in IF specimen

The curvature of both columns at the drift angle of 0.1% and 1.5% are shown in Fig. 9. As mentioned above, the lateral deformation of tensile column is restricted due to the remaining part of CB wall from the early stage to final stage of loading, which well corresponds to the crack patterns (Fig. 7(b)). This crack pattern well agrees with the high location (about $3/4h_0$ from the bottom) of inflection point in tensile column shown in Fig. 9. The moment distribution in both columns is therefore assumed as shown in the figure, and $h_0/2$ (h_0=610mm) is employed for the tensile column height, while h_0 is employed for the compression column herein. As a result, the total lateral strength calculated in both columns of this specimen is higher than that of BF specimen due to the short column effect by the partial height CB wall as shown in Fig. 6(b). The shear strength V_C of CB wall is then calculated according to Eqns. (4) and (5) (FEMA 306), and the sum of shear force of RC columns and CB wall is shown in Fig. 6(b), which does not show good agreement with the overall lateral strength.

$$V_C = a_{eq} \cdot t \cdot f_m \cdot \cos \theta_m \tag{4}$$

$$a_{eq} = 0.175 \cdot \left(\frac{4 \cdot E_c \cdot I_c \cdot h_m}{E_m \cdot t \cdot \sin 2\theta_m \cdot h^4} \right)^{0.1} \cdot l_d \tag{5}$$

where, a_{eq} is the equivalent strut width, t is the thickness of CB wall, f_m is the 50% of prism strength, θ_m is the angle of CB wall height to length, E_c is the Young's modulus of concrete, I_c is the moment of inertia of column, h_m is the height of CB wall, E_m is the Young's modulus of CB prism, h is the column height, and l_d is the diagonal length of CB wall, respectively.

4. EQIVALEN DIAGONAL STRUT AND SHEAR STRENGTH OF CB WALL

In this section, a modelling of the equivalent diagonal strut of CB wall is proposed based on the strain values of 3-axis strain gauges on CB units measured during the test. The shear load carried by the CB wall is then evaluated using the compressive stress acting in the equivalent diagonal strut width calculated from the element experiments of CB units which will be discussed later. In this paper, the proposed procedure at the drift angles of 0.2% and 0.67%, which correspond to the early stage and maximum strength drift angle, respectively, are representatively described in detail.

4.1. Modeling of Equivalent Diagonal Strut of CB Wall

The modeling of equivalent diagonal strut of CB wall including its main angle, equivalent width, and central axis is proposed and discussed as described in sections 4.1.1 through 4.1.5.

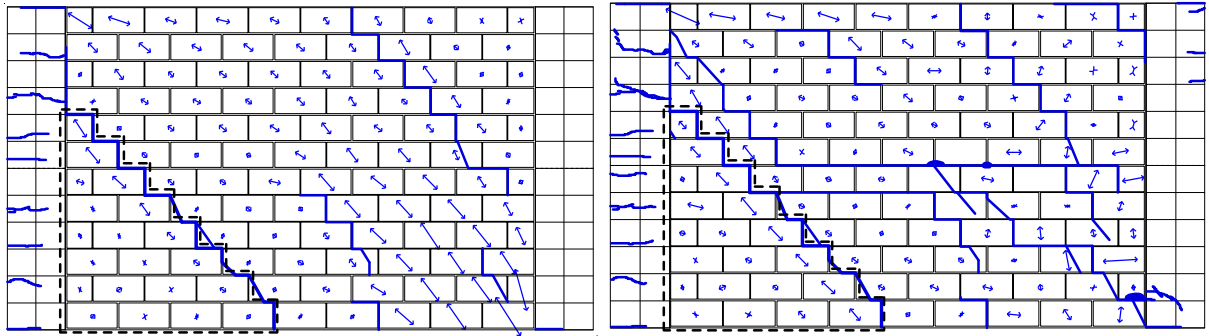### 4.1.1. Principal compressive strain and its angle of each CB unit

The principal compressive strain and its angle of each CB unit are first calculated according to the conventional Eqns. (6) through (8) from the strain values of 3-axis strain gauges on CB Wall. Figure 10 shows the principal compressive stain and its angle of each CB unit at the drift angle of 0.2% and 0.67%, respectively. As can be found in the figure, most principal compressive strain of CB units at the drift angle of 0.2% diagonally distributes with 45° in clockwise direction with respect to the horizontal line, while that at the peak drift angle of 0.67% shows more complicated distribution.

$$\varepsilon_{1,2} = \frac{\varepsilon_x + \varepsilon_y}{2} \pm \sqrt{\left(\frac{\varepsilon_x - \varepsilon_y}{2}\right)^2 + \left(\frac{\gamma_{xy}}{2}\right)^2} \tag{6}$$

$$\gamma_{xy} = 2\varepsilon_{xy} - (\varepsilon_x + \varepsilon_y) \tag{7}$$

$$\tan 2\theta_2 = \frac{\gamma_{xy}}{\varepsilon_x - \varepsilon_y} \tag{8}$$

where, ε_1 is the principal tensile strain, ε_2 is the principal compressive strain, ε_x and ε_y are diagonal direction strains on CB unit, ε_{xy} is the vertical direction strain of CB unit shown in Fig. 5, γ_{xy} is the shear strain, and θ_2 is the principal compressive strain angle with respect to the horizontal direction, respectively.

| (a) Drift angle of 0.2% | (b) Drift angle of 0.67% |

Figure 10. Principal compressive strain

4.1.2. Main diagonal strut angle of CB wall

The main diagonal strut angle representing the diagonal strut of CB wall is then estimated from the principal compressive strain and its angle of each CB unit. In this study, the average of the principal compressive angle weighted with its strain is employed to calculate the main diagonal strut angle θ as shown in Eqn. (9). As shown in the equation, strains ε_{2j} with angles between 0° and 90° are only employed. Note that the principal compressive strains and angles in the CB wall under the stair-stepped crack (enclosed by a dashed line in Fig. 10) are neglected, since it behaves as a partial height wall. From the calculation results, the main diagonal strut angle at drift angles of 0.2% and 0.67% are about 45° and 33°, respectively. The main diagonal strut angles have a decreasing tendency as the peak drift angle increases, and they are estimated to be in the range of about 30 to 45° at all peak drift angles throughout the test.

$$\theta = \left(\sum_{j=1}^{m} \varepsilon_{2j} \times \theta_{2j}\right) / \sum_{j=1}^{m} \varepsilon_{2j} \quad (0^0 \le \theta_{2j} \le 90^0) \tag{9}$$

where, ε_{2j} and θ_{2j} are principal compressive strain and angle of CB unit, and m is the number of CB units with θ_{2j} between 0° and 90°.

4.1.3. Principal compressive strain distribution along the diagonal strut

As shown in Fig. 11, the CB wall is divided to 15 sections at an equal interval in the diagonal direction,
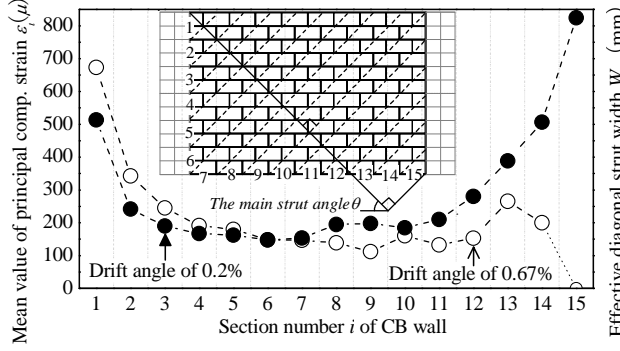
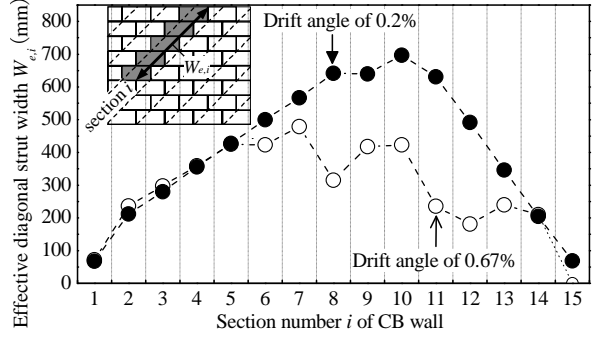**Figure 11.** Mean value of comp. strain in each section

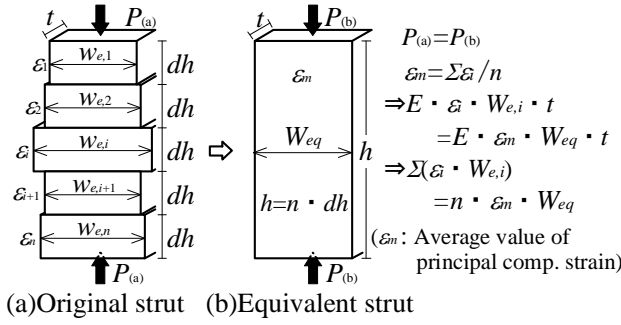**Figure 12.** Effective strut width in each section

(a)Original strut   (b)Equivalent strut

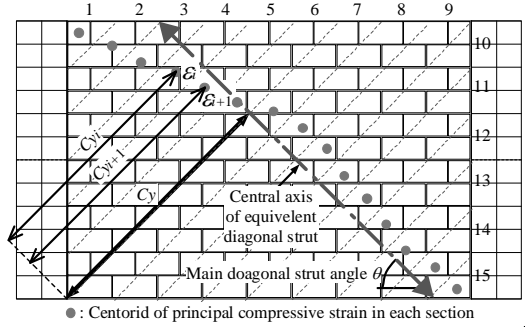**Figure 13.** Equivalent diagonal strut width

Figure 14. Central axis of diagonal strut

and the mean value of principal compressive strains ε_i of CB units included in section i (i=1 to 15) is calculated. The principal compressive strains with angles between 0° and 90° are only considered herein as is done earlier. As can be seen in the figure, the mean value shows nearly a symmetric distribution with concave shape at the drift angle of 0.2%, while it shows almost a symmetric distribution until section 13 but decreases in sections 14 and 15 at 0.67% drift, because some CB units are neglected in calculation due to their principal compressive angles smaller than 0° or larger than 90°. The average value of principal compression strain ε_m of 15 sections shown in Fig.11 is about 290µ and 220µ at 0.2% and 0.67% drift angle, respectively, and it distributes in the range of 290 to 190µ at all peak drift angles throughout the test.

4.1.4. Effective strut width and equivalent diagonal strut width
The effective strut width $W_{e,i}$ in each section is shown in Fig. 12, which is defined as the outmost distance of CB units having principal angle in the range of 0 to 90°. As shown in the figure, the effective strut width shows nearly a symmetric distribution with convex shape at the drift angle of 0.2%, but that at the drift angle of 0.67% decreases in some sections because the principal compressive angles of fewer CB units in those sections are in the range of 0 to 90°. The equivalent diagonal strut width W_{eq} is then evaluated according to Eqn. (10), which assumes that the same compression force P is applied to the equivalent strut section as shown in Fig 13. They are about 315 and 260mm at the drift angle of 0.2% and 0.67%, respectively. The equivalent strut width is evaluated to be in the range of 360 to 250mm at all peak drift angles throughout the test.

$$W_{eq} = \left(\sum_{i=1}^{n} (\varepsilon_i \times W_{e,i}) \right) / \sum_{i=1}^{n} \varepsilon_i \tag{10}$$

where, ε_i is the mean value of principal compressive strain and $W_{e,i}$ is the effective strut width in section i, and n is 15.

4.1.5. Central axis of diagonal strut
The distance of centroid Cy_i of principal compressive strain of CB units in section i is first calculated according to Eqn. (11) and they are plotted by ● in Fig. 14. The central axis of the diagonal strut C_y is then estimated according to Eqn. (12) and shown in the figure. Finally, the equivalent diagonal strut can be modelled as shown in Fig. 15.

$$Cy_i = \left(\sum_{j=1}^{m} \varepsilon_{2j} \times y_{2j} \right) / \sum_{j=1}^{m} \varepsilon_{2j} \tag{11}$$

$$Cy = \left(\sum_{i=1}^{n} \varepsilon_i \times Cy_i \right) / \sum_{i=1}^{n} \varepsilon_i \tag{12}$$

where, ε_{2j} is the principal compressive strains of CB units in section i, y_{2j} is the distance to each center of principal compressive strain in section i perpendicular to the main strut angle, ε_i is the mean value of principal compressive strain of CB units in section i, m is the number of CB units with θ_{2j} between 0° and 90° in section i, and n is 15.
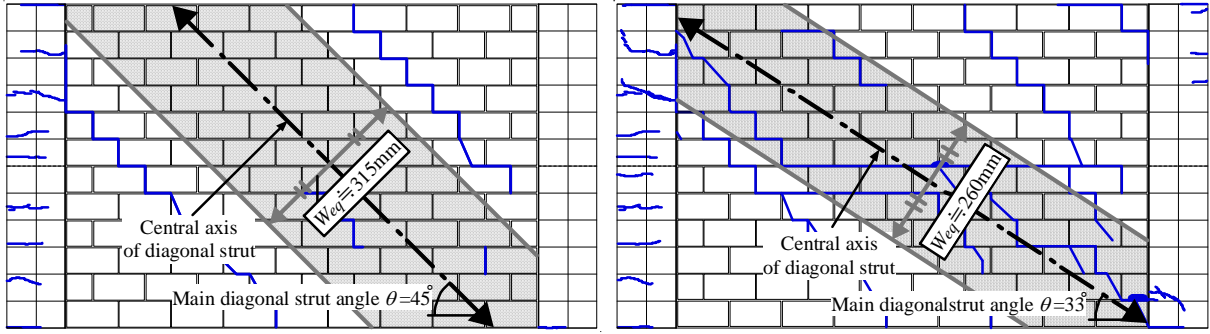
(a) Drift angle of 0.2%   (b) Drift angle of 0.67%

Figure 15 Modeling of Equivalent diagonal strut

4.2. Estimation of Shear Strength of CB Wall

In this section, the shear strength V_{cs} of CB wall is evaluated according to Eqn. (13) and the material test results of CB units. In the equation, σ_m is the principal compressive stress corresponding to the average principal compressive strain ε_m of equivalent diagonal strut, where ε_m is the average value obtained in section 4.1.3. In this paper, the stress (σ)-strain (ε) relationship with 45° compression loading, which is shown in Figs. 16 and 17, is employed for the σ_m-ε_m relationship to calculate the shear strength of CB wall as shown below.

$$V_{cs} = W_{eq} \cdot t \cdot \sigma_m \cdot \cos\theta \tag{13}$$

where, W_{eq} is the equivalent diagonal strut width, t is the wall thickness, σ_m is the compressive stress corresponding to the average compressive strain ε_m, and θ is the main diagonal strut angle, respectively.

(1) Compression tests of CB units with 90° and 0° uniaxial loadings are carried out, and their diagonal strains ε_a $(=(\varepsilon_{a1}+\varepsilon_{a2})/2)$ and ε_b $(=(\varepsilon_{b1}+\varepsilon_{b2})/2))$ are calculated (Fig. 16(a) and (b)).

(2) Diagonal strain ε_c $(=(\varepsilon_{ca}+\varepsilon_{cb})/2)$ by shear stress τ_c is obtained assuming the shear strains γ_{ca} and γ_{cb} equal to $\varepsilon_{ca}/\cos 45°$ and $\varepsilon_{cb}/\cos 45°$, respectively, and the shear modulus G_{ma} and G_{mb} are $0.4E_{ma}$ and $0.4E_{mb}$ (Young's modulus of CB unit), respectively, according to the reference (FEMA 273, 1997) (Fig. 16(c)).

(3) The strain ε is derived by the sum of these three diagonal strains ($\varepsilon = \varepsilon_a + \varepsilon_b + \varepsilon_c$), and the stress ($\sigma/2$) is then doubled as shown in Fig. 17 to obtain the σ_m-ε_m relationship.
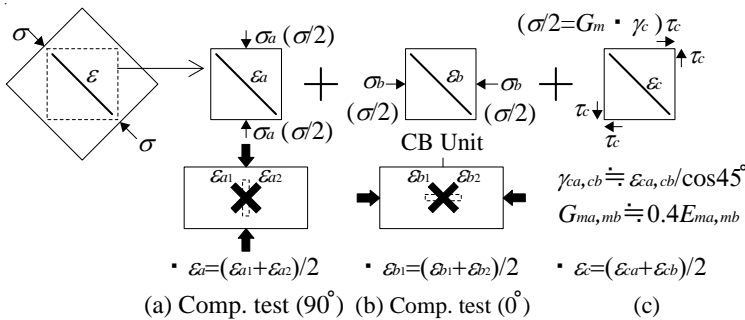

(a) Comp. test (90°)   (b) Comp. test (0°)   (c)

Figure 16. Assumption of stress-strain relationship at 45° loading   **Figure 17.** σ_m-ε_m relationship
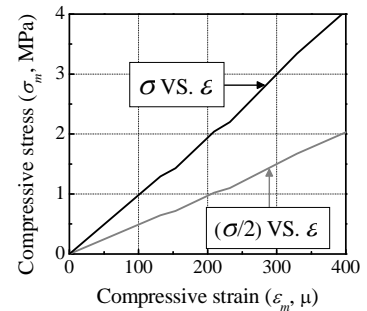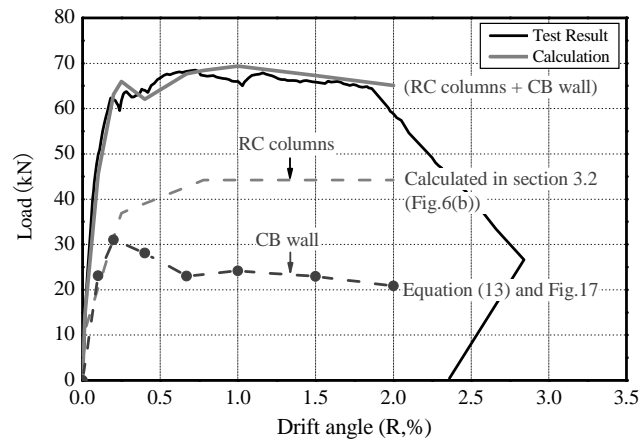
Figure 18. Lateral strength evaluation of IF specimen

The overall lateral load and deflection relationship of IF specimen is then demonstrated based on the estimated behavior of RC columns (Fig. 6(b)) and the lateral load V_{cs} carried by the CB wall from Eqn. (13) and Fig. 17. Figure 18 shows the calculated results where σ_m and corresponding V_{cs} are computed at the drift angles of 0.1, 0.2, 0.4, 0.67, 1.0, 1.5, and 2.0%. As can be seen in the figure, the proposed procedure shows successful agreement with overall lateral strength.

5. CONCLUSION

Seismic performance of RC frames with unreinforced CB wall for typical Korean school buildings was experimentally investigated under in-plane loadings. The major findings can be summarized as follows.

(1) BF specimen and IF specimen show different behavior against lateral loading, and RC columns in IF specimen has higher shear strength than BF specimen due to short column effect by the partial height CB wall.
(2) Calculation result of shear strength in BF specimen agrees well with recorded lateral strength. The sum of shear strength of RC columns and CB wall, which is employed in the reference (FEMA 306, 1998), however does not show good agreement with overall lateral strength in IF specimen.
(3) The modeling of equivalent diagonal strut of CB wall including its main angle, equivalent width, and central axis is proposed. Shear load carried by CB wall is then evaluated based on compressive stress acting on the equivalent diagonal strut width calculated from the element experiments of CB units. The evaluation results of shear strength by the sum of both RC columns and CB wall shows successful agreement with the overall lateral strength recorded in IF specimen.

REFERENCES

The Ministry of Construction and Transportation. (2002). A Study on the Seismic Evaluation and Retrofit of Low-Rise RC Buildings in Korea (in Korean).
FEMA 306. (1998). Evaluation of Earthquake Damaged Concrete and Masonry Wall Buildings. Applied Technology Council (ATC-43 Project).
Architectural Instite of Japan (AIJ). (2010). AIJ Standard for Structural Calcuation of Reinforced Concerete Structures.
Architectural Instite of Japan (AIJ). (1988). AIJ Standard for Structural Calcuation of Reinforced Concerete Structures.
FEMA 273. (1997). NEHRP Guidelines for the seismic rehabilitation of buildings (ATC-33 Project).